DOI: 10.61782/fa.2023.0961

forum acusticum 2023

PRACTICAL FORMULAS FOR QUANTIFYING THE UNCERTAINTY OF AIRBORNE SOUND INSULATION MEASUREMENTS CAUSED BY THE DIFFUSE FIELD ASSUMPTION

Edwin Reynders*

Department of Civil Engineering, Faculty of Engineering Science, KU Leuven, Belgium

ABSTRACT

In the conventional approach for experimental airborne sound insulation assessment, as standardized in ISO 10140-2, it is (implicitly) assumed that the sound fields in the source and receiver rooms are diffuse. A diffuse field is by definition a random field: it represents a conceptual ensemble of rooms with the same volume and total absorption, but otherwise any possible arrangement of boundaries and objects that scatter incoming sound waves. Adopting a diffuse sound field model in the assessment procedure therefore inherently introduces uncertainty on the resulting ratings, such as the weighted sound reduction index and the spectrum adaptation terms from ISO 717-1. When determining such quantities in one particular transmission suite, this uncertainty is important below the highest Schroeder frequency of both rooms. In this work, closed-form expressions are presented for quantifying the uncertainty on experimentally determined sound reduction indices and related single-number ratings that is due to the diffuse field assumption when measurements are carried out in one particular transmission suite. They are numerically validated and their practical use is demonstrated in applications. They can be easily incorporated into overall uncertainty assessment procedures such as the detailed uncertainty budget analysis of ISO 12999-1.

Keywords: *building acoustics, airborne sound insulation, measurement uncertainty, uncertainty budget*

**Corresponding author*: edwin.reynders@kuleuven.be.

1. INTRODUCTION

The experimental assessment and rating of the airborne sound insulation of individual building elements such as walls and floors is crucial for designing buildings with sufficient noise protection. However, such an assessment faces difficulties, since the airborne sound insulation of a particular wall type depends on its dimensions and boundary conditions as well as on the properties of the sound fields at the source and receiver sides [1]. For this reason, standardized assessment procedures are used, in which the wall is tested in a laboratory with suppressed flanking transmission and a sufficiently large opening and the sound fields in the source and receiver rooms are taken to be diffuse. An example of such as procedure can be found in ISO 10140-2 [2] which is complemented with ISO 717-1 [3] for generating single-number ratings. The diffuse field assumption is a crucial element of this procedure, because it needs to be satisfied to ensure (i) that the computation of the airborne sound insulation values from the measured spatially averaged sound pressure levels is correct, and (ii) that the results do not depend on the geometry and dimensions of the rooms.

The validity of the diffuse field assumption is frequency dependent. Above the Schroeder frequency of a room, its modal overlap is considered sufficiently high, such that its sound field can be well approximated as diffuse, irrespective of the excitation and the room details [4]. This implies that well below the Schroeder frequency, the sound insulation of a building element may differ significantly from situation to situation, i.e., it may change considerably when different source and receiver rooms are considered, even if all other variables are kept constant. This has been confirmed in several numerical studies such

as [5] and [6] as well as in a series of interlaboratory tests, an overview of which can be found in [7].

However, a diffuse field is by definition a random field: it represents a conceptual ensemble of rooms with the same volume and total absorption, but otherwise any possible arrangement of boundaries and objects that scatter incoming sound waves. Adopting a diffuse sound field model in the assessment procedure therefore inherently introduces uncertainty on the results. That uncertainty is small above the Schroeder frequency, so the diffuse field model is essentially deterministic at high frequencies. Below the Schroeder frequency, a diffuse field model can still be valid but in an ensemble sense rather than for one particular room-wall-room system. Recent theoretical studies have extended diffuse sound transmission models such that not only the ensemble mean, but also the ensemble variance and the complete probability distribution of the diffuse airborne sound insulation can be computed [8, 9]. These studies have also confirmed, by means of detailed numerical simulation, that the related theoretical values of the mean, variance and probability distribution correspond to observed sound insulation values across an ensemble of transmission suites, also at frequencies far below the Schroeder frequencies of the rooms, as long as the variability across that ensemble is sufficiently large.

It would be very interesting if one could quantify the diffuse field uncertainty on measured sound insulation data obtained in a specific test facility, especially below the Schroeder frequencies, as this would allow to assess to what extent these data are reproducible in other test facilities when the other parameters (such as transmission opening dimensions) remain unchanged. It is also an essential element when deriving a detailed uncertainty budget of the total measurement uncertainty, as foreseen in ISO 12999-1 [10]. However, until now this has been an open problem, such that uncertainty quantification of sound insulation laboratory measurements has been based on inter-laboratory (or round robin) tests [7,10]. Although essential for validation purposes, these tests are expensive and time-consuming, such that inter-laboratory data are available for only a few wall types.

In the present work, such an uncertainty quantification if developed. It starts from the observation that the relevant closed-form expression that was derived for the band-averaged variance of the airborne sound insulation of a wall caused by the diffuse field assumption in [9], only depends on quantities that are readily available in conventional sound insulation tests such as ISO 10140-2 [2]. These results are first discussed and then employed to derive a practical uncertainty assessment for the single-numer ratings of the airborne sound reduction index that appear in the ISO 717-1 standard [3]. The accuracy of the expressions is investigated in a Monte Carlo simulation study and their practical use in experiments is illustrated.

2. VARIANCE OF BAND-AVERAGED DIFFUSE SOUND REDUCTION INDEX

The transmission loss R across a partition wall, also known as its airborne sound insulation or sound reduction index, is determined by the sound transmission coefficient τ_{12}. For a given sound power $P_{\mathrm{inc}}^{(1)}$ that is incident upon the wall in the source room (numbered room 1 from here on), the transmission coefficient is defined as the ratio of the power flow $P_{\mathrm{in}}^{(1\to2)}$ from the source room to the receiver room (numbered room 2 from here on), to $P_{\mathrm{inc}}^{(1)}$. In engineering practice, the sound insulation is usually evaluated in frequency bands $\Delta := [\omega_{\mathrm{l}}, \omega_{\mathrm{u}}]$ with nominal center frequency ω_{c}. This results in the band-averaged transmission loss which is defined as

$$R_{\Delta}(\omega_{\mathrm{c}}) := -10 \log \tau_{12,\Delta}(\omega_{\mathrm{c}}), \tag{1}$$

where the band-averaged transmission coefficient equals

$$\tau_{12,\Delta}(\omega_{\mathrm{c}}) := \frac{\int_{\omega_{\mathrm{l}}}^{\omega_{\mathrm{u}}} P_{\mathrm{in}}^{(1\to2)}(\omega)\mathrm{d}\omega}{\int_{\omega_{\mathrm{l}}}^{\omega_{\mathrm{u}}} P_{\mathrm{inc}}^{(1)}(\omega)\mathrm{d}\omega}. \tag{2}$$

In order to avoid ambiguity, it is typically assumed that $P_{\mathrm{inc}}^{(1)}(\omega)$ be constant in each frequency band.

As discussed in Sec. 1, the transmission loss depends on the sound fields in the source and receiver rooms. If these are modeled as diffuse, they are random and so is the transmission loss. It has been recently demonstrated, both theoretically and by means of detailed simulation, that the variance of the transmission coefficient which is due to the diffuse field assumption equals [9]

$$\frac{\mathrm{Var}\left[\tau_{12,\Delta}\right]}{\hat{\tau}_{12,\Delta}^2} \approx \frac{b_1}{N} + \frac{a_2}{\pi m_2}\left(b_{2\mathrm{R}1} + \frac{b_2}{N}\right). \tag{3}$$

In this expression, N is the number of wall modes that contribute to the sound transmission, m_2 is the modal overlap factor of the receiver room, a_2 is the diffuse field correction factor and b_1, b_2 and $b_{2\mathrm{R}1}$ are bandwidth factors. The physical meaning and the computation of these variables is discussed below. The approximation in

Eq. (3) holds for the case of light fluid loading (meaning that the wall impedance is much larger than the radiation impedance of air, which holds for the considered building acoustics applications) and when the energy dissipation in the receiver room is not dominated by sound transmission through the wall (which is also generally the case except when the wall has extremely low sound insulation). In case the approximation would not be accurate, more general results which are also presented in [9] can be employed.

The modal overlap factor of a homogeneous system component is defined as

$$m := \omega \eta n, \tag{4}$$

with η the damping loss factor and n the modal density. The modal overlap factor of the receiver room m_2 therefore requires the knowledge of its damping loss factor η_2 and modal density n_2 at the (band center) frequencies of interest. The damping loss factor relates directly to the reverberation time T:

$$\eta = \frac{4.4\pi}{\omega T}. \tag{5}$$

The modal density of the receiver room can be readily obtained from its geometry; the leading term depends on its volume V_2 only [11, Eq. 8.3.5]:

$$n_2 = \frac{V_2 \omega^2}{2\pi^2 c^3}, \tag{6}$$

where c denotes the sound speed.

The number of wall modes N which contribute to the sound transmission at a given frequency can be estimated as [9, Eq. 45]

$$N \approx 1 + \pi m_\mathrm{w}, \tag{7}$$

where m_w denotes the modal overlap factor of the wall. The damping loss factor of the wall η_w can be obtained from a structural reverberation test and employing (5). The estimation of the modal density requires the wave and phase speeds of the wall; practical expressions e.g. for thin plates in bending are available from e.g. [11, Sec. 8.2]. If the estimation of either η_w or n_w is not practically possible, one can make use of the fact that N is bounded below by unity:

$$1 \leq N. \tag{8}$$

Employing the approximation $N \approx 1$ then yields an upper bound on the transmission loss variance.

The diffuse field correction factor a_2 accounts for the fact that the variance of the diffuse field in the receiver room depends on the excitation. It depends only on the quantities m_2 and N which were discussed above:

$$a_2 = 1 + \frac{2 + \mathrm{q}(m_2)}{N}, \tag{9}$$

where the function $\mathrm{q}(m)$ is defined as

$$\mathrm{q}(m) := \mathrm{q}_1(m) + \mathrm{q}_2(2) \tag{10}$$

$$\mathrm{q}_1(m) := -1 + \frac{1}{2\pi m}\left(1 - \exp(-2\pi m)\right) \tag{11}$$

$$\mathrm{q}_2(m) := \mathrm{E_i}(\pi m)\left(\cosh(\pi m) - \frac{\sinh(\pi m)}{\pi m}\right). \tag{12}$$

The function $\mathrm{E_i}$ denotes the exponential integral which requires numerical evaluation. If needed, the following approximations can be employed:

$$\mathrm{q}(m) \to \mathrm{q}_1(m), \quad m \to 0 \tag{13}$$

$$\mathrm{q}(m) \to -1 + \frac{1}{\pi m}, \quad m \to \infty. \tag{14}$$

The bandwidth factors b_1, b_2 and $b_{2\mathrm{R}1}$ depend only on the relative bandwidth and the loss factors of the rooms. They combine into a single variable for each room j:

$$B_j := \frac{\omega_\mathrm{u} - \omega_\mathrm{l}}{\omega_\mathrm{c} \eta_j} = \frac{\omega_\mathrm{u} - \omega_\mathrm{l}}{4.4\pi} T_j. \tag{15}$$

The bandwidth factors themselves are defined as follows:

$$b_j := \frac{-1}{B_j^2} \ln\left(1 + B_j^2\right) + \frac{2}{B_j} \operatorname{atan}\left(B_j\right) \tag{16}$$

and

$$B_j := \frac{\omega_\mathrm{u} - \omega_\mathrm{l}}{\omega \eta_j} \tag{17}$$

$$b_{2\mathrm{R}1} := \delta_{1j} \frac{\operatorname{atan}\left(B_2\right)}{B_2}, \quad B_1 = B_2 \tag{18}$$

$$:= \frac{B_1^2 b_1 - B_2^2 b_2}{B_1^2 - B_2^2}, \quad B_1 \neq B_2. \tag{19}$$

All variables that appear in the difuse transmission coefficient variance expression (3) have now been discussed in detail. From (3), the variance of the diffuse transmission loss can be obtained as

$$\mathrm{Var}\left[R_\Delta\right] = \frac{100}{\ln 10} \log\left(1 + \frac{\mathrm{Var}\left[\tau_{12,\Delta}\right]}{\hat{\tau}_{12,\Delta}^2}\right). \tag{20}$$

As argued in [9], this expression follows from the fact that the probability distribution of the transmission coefficient

τ_{12} is proportial to the probability distribution of the transmitted power $P_{\text{in}}^{(1\to2)}$, which in its turn is very well approximated by a lognormal distribution. It then follows immediately that the transmission loss R is normally distributed, a fact which can be used e.g. for computing confidence intervals of R from its mean and variance.

3. VARIANCE OF SINGLE-NUMBER RATINGS

In this section, it is illustrated how the above theory can be used for practical uncertainty assessment regarding the single-numer ratings of airborne sound insulation that appear in ISO 717-1 [3]. The methodology is readily generalized to other ratings, either standardized or not.

3.1 Weighted sound reduction index

If the sound reduction index R_Δ has been determined in 1/3 octave or 1/1 octave bands covering the frequency range from 100 to 3150 Hz, the corresponding weighted sound reduction index R_{w} can be computed by comparison against a reference curve. Mathematically, R_{w} is implicitly defined, as the variable for which the following equality holds:

$$\sum_{j=1}^{n_{\text{b}}} \max(R_{\text{w}} + a_j - R_{\Delta j}, 0) = 2n_{\text{b}}, \tag{21}$$

where a_j is the difference between the value of the reference curve from [3, Table 3] and its value at 500 Hz (52 dB) and n_{b} denotes the number of frequency bands (e.g. $n_{\text{b}} = 16$ for 1/3 octave band data). The maximum which appears in the above equation is not differentiable, but for instance the following approximation can be employed

$$\max(x, 0) \approx \frac{1}{\alpha} \ln\left(1 + \exp\left(\alpha x\right)\right), \tag{22}$$

where α is a sharpness parameter. The approximation error is smaller than $\ln(2)/\alpha$. For example, if $\alpha = 70$ then the error is smaller than 0.01 dB. With this approximation, (21) transforms into

$$\sum_{j=1}^{n_{\text{b}}} \ln\left(1 + \mathrm{e}^{\alpha x_j}\right) = 2n_{\text{b}}\alpha, \tag{23}$$

where x_j is defined as

$$x_j := R_{\text{w}} + a_j - R_{\Delta j}. \tag{24}$$

By differentiating both sides of (23) to $R_{\Delta j}$, one finds that

$$\frac{\partial R_{\text{w}}}{\partial R_{\Delta j}} = \frac{\mathrm{e}^{\alpha x_j}}{1 + \mathrm{e}^{\alpha x_j}} \left(\sum_{j=1}^{n_{\text{b}}} \frac{\mathrm{e}^{\alpha x_j}}{1 + \mathrm{e}^{\alpha x_j}} \right)^{-1} \tag{25}$$

Whent the bandwidth is large enough, it is reasonable to assume that the $R_{\Delta j}$ are uncorrelated hence statistically independent (since they are normally distributed). The variance of the single-number rating may then be approximated as

$$\operatorname{Var}\left[R_{\text{w}}\right] \approx \sum_{j-1}^{n_{\text{b}}} \left(\frac{\partial R_{\text{w}}}{\partial R_{\Delta j}} \right)^2 \operatorname{Var}\left[R_{\Delta j}\right]. \tag{26}$$

3.2 Spectrum adapted sound reduction indices

ISO 717-1 also contains a second, fundamentally different procedure for obtaining a single-number rating. It relates to the overall A-weighted sound pressure level at the receiver side of the wall for a fixed source spectrum. The corresponding rating $R_{\text{A}s}$ is defined as

$$R_{\text{A}s} := -10 \log \sum_{j=1}^{n_{\text{b}}} 10^{\frac{L_{js} - R_{\Delta j}}{10}}, \tag{27}$$

where L_{js} is spectrum number s from [3, Table 4 or B.1]. It then follows immediately that

$$\frac{\partial R_{\text{A}s}}{\partial R_{\Delta j}} = 10^{\frac{L_{js} - R_{\Delta j} + R_{\text{A}s}}{10}}. \tag{28}$$

Similar considerations as for R_{w} then lead to

$$\operatorname{Var}\left[R_{\text{A}s}\right] \approx \sum_{j-1}^{n_{\text{b}}} \left(\frac{\partial R_{\text{A}s}}{\partial R_{\Delta j}} \right)^2 \operatorname{Var}\left[R_{\Delta j}\right]. \tag{29}$$

This is a known result which has been obtained e.g. in [12] in a slightly different form.

4. NUMERICAL VERIFICATION

In this section, the validity of the previous analysis is numerically verified for a particular room-wall-room system. This example system has previously appeared in [9] but it is extended here to include single-number ratings. The wall is made of gypsum blocks (Young's modulus $E = 3.15$ GPa, Poisson's ratio $\nu = 0.2$, mass density $\rho = 910\ \frac{\text{kg}}{\text{m}^3}$, loss factor $\eta = 0.03$) and measures 3.25 by 2.95 by 0.10 m. It is modeled as a simply supported

thin Kirchhoff-Love plate. The geometry of the source and receiver rooms is depicted in Fig. 1. The source room is excited by a monopole source, the location of which is also indicated in Fig. 1. Both rooms have a reverberation time of 1.5 s and the sound speed is 343 m/s.

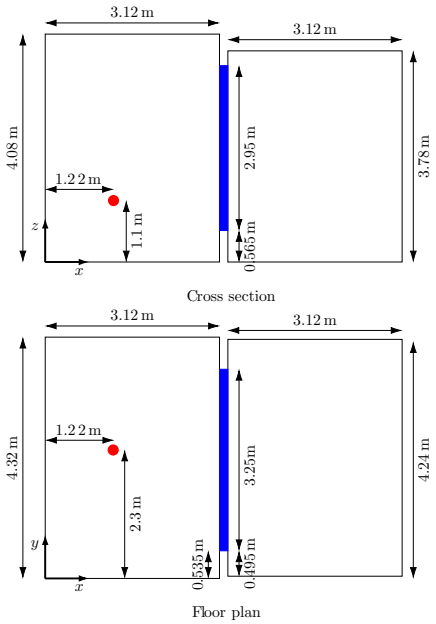

Figure 1. Geometry of the room–wall–room configuration and monopole source location.

The rooms are random in the sense that in each room, a total of 30 acoustic point masses, each of which has 0.4 % of the total acoustic mass V/c^2 of the room, are distributed at random locations. Note that the total number of air pockets and their individual acoustic mass have been arbitrarily chosen; the important point is that, from a certain frequency onwards, the randomness caused by the wave scatterers is expected to reach a state of maximum information entropy, which conforms to a diffuse field.

The statistics of the sound transmission loss which follow from the detailed Monte Carlo simulation are then compared to those of the diffuse transmission loss. The mean diffuse transmission loss of the baffled wall is computed from [9, Eq. 20]. In this way, its finite size and boundary conditions are rigorously accounted for. The variance of the transmission loss is computed as detailed in Sec. 2.

In Fig. 2, the mean and standard deviation of the airborne sound insulation as obtained from the Monte Carlo simulation are compared with the diffuse values. Both harmonic results and results in 1/3 octave bands are displayed. At very low frequencies, the local harmonic sound fields in the rooms are insufficiently sensitive to the presence of the small acoustic point masses that have been introduced in the detailed Monte Carlo model, for reaching a diffuse field. This is most clearly visible in the standard deviation plots: at very low frequencies, the variance is over-estimated by the diffuse field model, while at higher frequencies, it accurately predicts the sound insulation variance. Nevertheless, it is also visible in the harmonic mean plot: at very low frequencies, individual plate and room modes have a clear influence on the ensemble average sound insulation, but the diffuse field model only picks up the individual plate modes. When the frequency increases, the natural frequencies of the rooms start to mix well across the random ensemble, resulting in a good match between the mean transmission losses as predicted from the detailed and diffuse models. The frequency at which the Monte Carlo results and the diffuse results start to match can be lowered by considering a more random ensemble. Finally, it can be noted that the approximation $N \approx 1$ yields a reasonable but conservative upper bound on the variance, as expected.

In table 1, the mean and standard deviations of some single-number ratings from ISO 717-1 as obtained from the Monte Carlo simulation are compared with the diffuse values. The Monte Carlo simulation results do not include 1/3 octave results above 500 Hz as the related detailed modal simulation model becomes computationally very expensive at high frequencies. For this reason, only

Table 1. Mean values and 95 % confidence intervals of the single-numer ratings R_w, $R_\mathrm{A} = R_\mathrm{A1} = R_\mathrm{w} + C$ and $R_\mathrm{Atr} = R_\mathrm{A2} = R_\mathrm{w} + C_\mathrm{tr}$ as obtained by Monte Carlo simulation for an ensemble of room-wall-room systems and the corresponding diffuse values.

rating	Monte Carlo	diffuse
$R_{\mathrm{w},100-500}$ [dB]	36.20 ± 0.75	36.28 ± 0.63
$R_{\mathrm{A},100-500}$ [dB]	38.53 ± 0.69	38.75 ± 0.57
$R_{\mathrm{Atr},100-500}$ [dB]	35.77 ± 0.71	36.25 ± 0.57

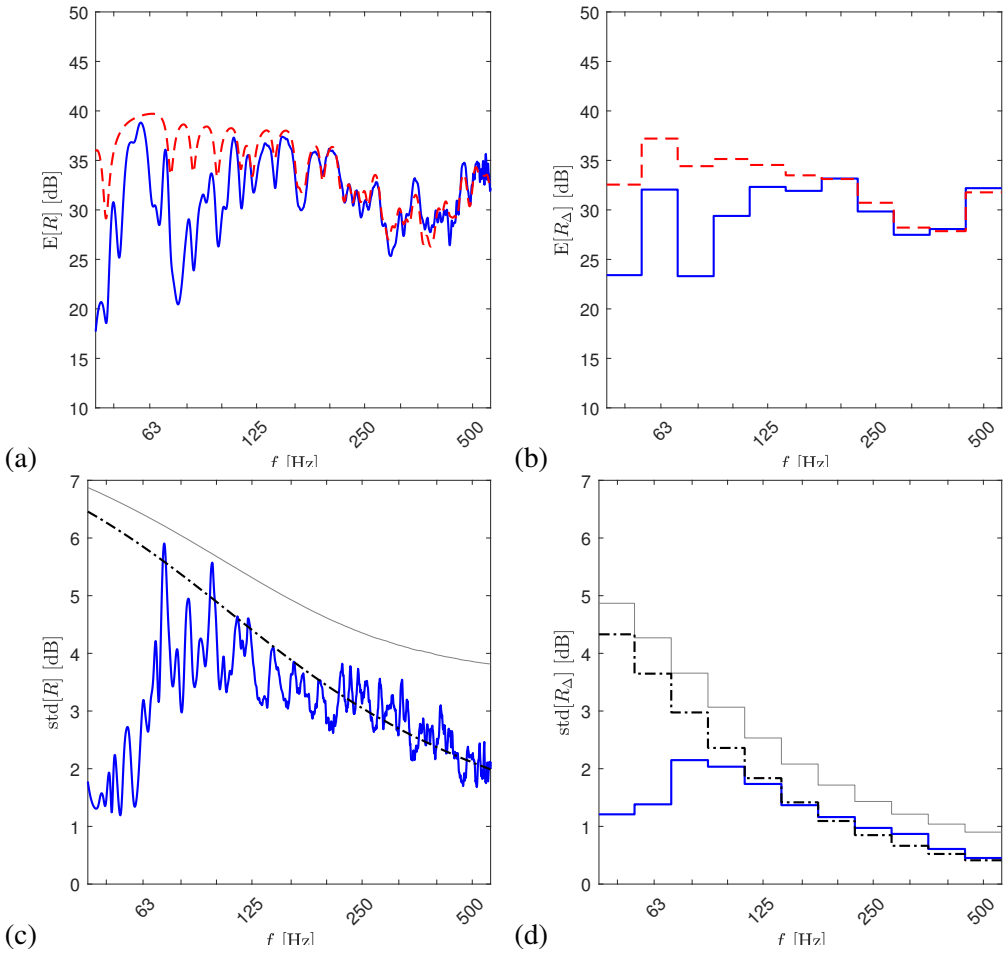

Figure 2. Mean (a-b) and standard deviation (c-d) of a room-wall-room system with acoustic point masses at random locations in the rooms. (a,c): harmonic results, (b,d) 1/3 octave band results. Blue: Monte Carlo simulations; Red dashed lines: mean diffuse values; black dash-dotted lines: exact diffuse standard deviations; thin grey lines: diffuse standard deviations with $N \approx 1$.

the 1/3 octave bands up to 500 Hz have been employed for the computation of R_w and $R_{\mathrm{A}s}$. This implies e.g. that in Eq. (21) and following, $n_\mathrm{b} = 8$ has been used. The values of the reference curve and sound level spectra of ISO 717-1 have been adopted without modification for the reduced frequency range analysis. Both the average values and the standard deviations σ (or, equivalently, the $\pm 2\sigma$ confidence intervals) across the considered random ensemble agree well with the diffuse values.

5. PRACTICAL EXAMPLES

In order to illustrate the practical use of the presented expressions, they are applied here to quantify the diffuse field uncertainty of the measured airborne sound insulation of two cavity walls. The leafs of the first cavity wall consists of a single sheet of $15\,\mathrm{mm}$ fire-resistant plasterboard. They are connected to regular C-shaped metal studs with a steel thickness of $0.6\,\mathrm{mm}$. The stud spacing is $60\,\mathrm{cm}$. The cavity has a depth of 75 mm and it is filled with 60 mm glass wool. The second cavity wall is identical to the first one, except that the leafs each contain a second sheet of plasterboard. The walls were tested in the KU Leuven Laboratory of Acoustics. The source and receiver room both have a volume of 87 m^3. The transmission opening has a width of 3.25 m and a height of 2.95 m.

Fig. 3 displays the measured sound reduction index of both walls, together with the 95 % confidence intervals that have been computed from Eq. (20) using the geometrical room parameters detailed above and the measured room reverberation times. The modal density of the wall has been estimated by taking the modal density of a single sheet of plasterboard with nominal material properties (longitudinal wave speed 1800 m/s and loss factor 0.03). The confidence intervals indicate how well the measurement results would carry over to any other laboratory, if only the room geometries would be different.

It can be observed in Fig. 3 that for both walls, the nominal (i.e., ensemble-averaged) single-numer rating $\hat{R}_\mathrm{w}$ is determined by the sound reduction index at low frequencies as well as in the highest frequency bands, where the coincidence dip is clearly present: in both frequency regions, R is below the shifted reference curve. However, there is a clear difference betwee both walls: for single sheeting the sound reduction index crosses the reference curve at 200 Hz while for double sheeting this happens above 400 Hz. As the diffuse field uncertainty is the highest at the lowest frequencies, it can therefore be expected that the uncertainty of R_w is larger for the wall with single sheeting than for the wal with double sheeting.

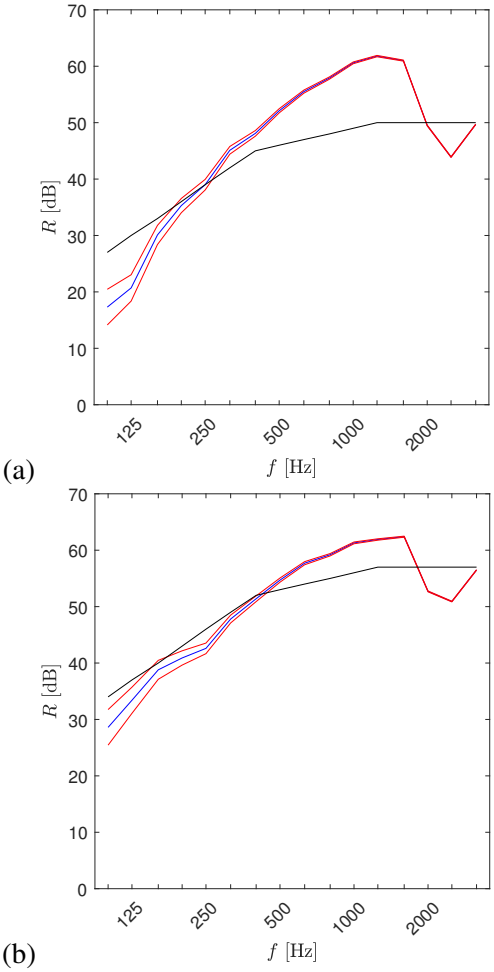

Figure 3. Sound reduction index of a cavity wall with (a) single sheets and (b) double sheets of plasterboard. Blue curves: measured (nominal, mean) values $\hat{R}$; red curves: 95,% confidence interval due to the diffuse field assumption; black curves: shifted reference curves corresponding to $\hat{R}_\mathrm{w}$.

This is confirmed in Table 2, where the single-numer ratings and their 95 % confidence intervals are listed. It is also clear that the uncertainty of $R_\mathrm{w} + C_\mathrm{tr}$ is the largest as this rating gives more weight to the lower frequency bands.

Table 2. Single-numer ratings of the plasterboard walls and their uncertainties, expressed as 95 % confidence intervals, due to the diffuse field assumption.

rating	single sheets	double sheets
R_w [dB]	46.3 ± 0.6	53.4 ± 0.5
$R_\mathrm{w} + C$ [dB]	42.0 ± 1.4	51.0 ± 0.9
$R_\mathrm{w} + C_\mathrm{tr}$ [dB]	35.2 ± 2.0	45.7 ± 1.7

6. CONCLUSIONS

In this article, closed-form expressions have been presented for estimating the uncertainty of the sound reduction index of a wall or floor as determined in a transmission suite that is associated with the assumption of diffuse sound fields in the source and receiver rooms. Eq. (20) and the related expressions enable to estimate the uncertainty of harmonic or band-averaged values. They reveal that the uncertainty decreases with increasing room volumes, room reverberation times, bandwidth and wall modal density. The uncertainty of single-numer ratings can be estimated as detailed in Sec. 3. The accuracy of the expressions has been confirmed in a Monte Carlo simulation study and their practical use has been demonstrated using measured laboratory data.

7. ACKNOWLEDGMENTS

This work was funded by the European Research Council under ERC Starting Grant 714591 VirBAcous.

8. REFERENCES

[1] C. Hopkins, *Sound insulation*. Oxford: Elsevier Ltd., 2007.

[2] International Organization for Standardization, *ISO 10140-2: Acoustics – Laboratory measurement of sound insulation of building elements – Part 2: Measurement of airborne sound insulation*, 2010.

[3] International Organization for Standardization, *ISO 717-1: Acoustics – Rating of sound insulation in buildings and of building elements – Part 1: Airborne sound insulation*, 2020.

[4] M. Schroeder, "The "Schroeder frequency" revisited," *Journal of the Acoustical Society of America*, vol. 99, no. 5, pp. 3240–3241, 1996.

[5] W. Kropp, A. Pietrzyk, and T. Kihlman, "On the meaning of the sound reduction index at low frequencies," *Acta Acustica*, vol. 2, no. 5, pp. 379–392, 1994.

[6] A. Osipov, P. Mees, and G. Vermeir, "Low-frequency airborne sound transmission through single partitions in buildings," *Applied Acoustics*, vol. 52, no. 3–4, pp. 273–288, 1997.

[7] V. Wittstock, "Determination of measurement uncertainties in building acoustics by interlaboratory tests. Part 1: airborne sound insulation," *Acta Acustica united with Acustica*, vol. 101, no. 1, pp. 88–98, 2015.

[8] E. Reynders, R. Langley, A. Dijckmans, and G. Vermeir, "A hybrid finite element - statistical energy analysis approach to robust sound transmission modelling," *Journal of Sound and Vibration*, vol. 333, no. 19, pp. 4621–4636, 2014.

[9] E. Reynders and C. Van hoorickx, "Uncertainty quantification of diffuse sound insulation values," *Journal of Sound and Vibration*, vol. 544, no. 117404, pp. 1–15, 2023.

[10] International Organization for Standardization, *ISO 12999-1:2014: Acoustics – Determination and application of measurement uncertainties in building acoustics – Part 1: Sound insulation*, 2014.

[11] R. Lyon and R. DeJong, *Theory and application of statistical energy analysis*. Newton, MA: Butterworth-Heinemann, second ed., 1995.

[12] V. Wittstock, "On the uncertainty of single-number quantities for rating airborne sound insulation," *Acta Acustica united with Acustica*, vol. 93, no. 3, pp. 375–386, 2007.